Quantitative Characterization of Marble Natural Aging through Pore Structure Image Analysis

Stability of a III-V/Si hybrid laser with a frequency-selective SiN mirror

Cristina Rimoldi[a], Lorenzo L. Columbo[a], Jock Bovington[b], Sebastian Romero García[c], Dominic Siriani[b], and Mariangela Gioannini[a]

[a]Dipartimento di Elettronica e Telecomunicazioni, Politecnico di Torino, Italy
[b]Cisco Systems, San José, CA, USA
[c]Cisco Optical, Nuremberg, Germany

ABSTRACT

We study the stability of a hybrid laser source consisting of a III-V reflective semiconductor optical amplifier (RSOA) edge-coupled to a silicon photonic mirror, based on two coupled high-Q microring resonators, providing a narrow band effective reflectivity. We simulate the laser dynamics through a model of time-delayed algebraic equations accounting for the frequency-selective mirror reflectivity, demonstrating single-mode emission, self-pulsing, and turbulent regimes. Further, we identify the regions of higher CW operation in terms of bias current and laser detuning with respect to the reflectivity peak. Finally, we test the CW laser stability with respect to optical feedback, mimicking the effect of spurious back-reflections from the passive parts of the circuit, and demonstrate ultra-stable CW operation for a sizeable range of detuning.

Keywords: Silicon photonic design, semiconductor lasers, optical feedback tolerance

1. INTRODUCTION

In recent years, silicon photonic (SiPh) integrated lasers have gained increasing traction for the realization of low-cost mass-producible devices for applications in telecommunications (e.g., optical transmitters), sensing, and metrology (e.g., LIDAR). These laser structures usually consists of a RSOA based on a III-V gain medium coupled to a silicon photonic circuit, providing the external laser cavity mirror. Several design solutions can be considered for the SiPh circuit, including but not limited to the use of passive components such as micro-rings, DBR reflectors, delay lines, and Mach-Zehnder interferometric configurations. As a result, lasers exploiting this technology with very narrow linewidth and wide tunability have been experimentally realized.[1–4]

While the reduction of the laser CW linewidth in these structures has been extensively studied both from an experimental and theoretical point of view,[4,5] few works have been dedicated to the analysis of the laser dynamical behavior in more complex regimes. This is of particular importance when considering silicon photonic mirrors with a very narrow bandwidth (i.e. of a few GHz) and therefore highly dispersive in amplitude and phase, as achievable e.g. through the integration of high-Q micro-rings.[6] Another issue, extremely relevant for possible application of these sources in the context of telecommunications, is represented by the laser sensitivity to spurious back-reflections from the passive parts of the silicon photonic circuit. In this context, isolator-free operation and laser design with high tolerance to optical feedback are sought with interest by the industry.

In this contribution, we report on the application of a theoretical model,[7] properly accounting for mirror dispersion, to describe the complex multimode dynamics of a typical SiPh hybrid laser and to address the issue about the laser sensitivity to optical feedback. Numerical simulations show a variety of possible regimes in solitary laser operation depending on the position of the CW lasing emission frequency with respect to the SiPh mirror reflectivity peak, ranging from ultra-stable cases, where the laser relaxation oscillations are highly damped, to self-pulsing and turbulent regimes. Further, the impact of the narrow band reflector, the linewidth enhancement

Further author information:
C.R., L.L.C, M.G. (postal address): corso Duca degli Abruzzi 24, Torino, IT-10129, Italy
C.R. (e-mail): cristina.rimoldi@polito.it
L.L.C. (e-mail): lorenzo.columbo@polito.it
M.G. (e-mail): mariangela.gioannini@polito.it

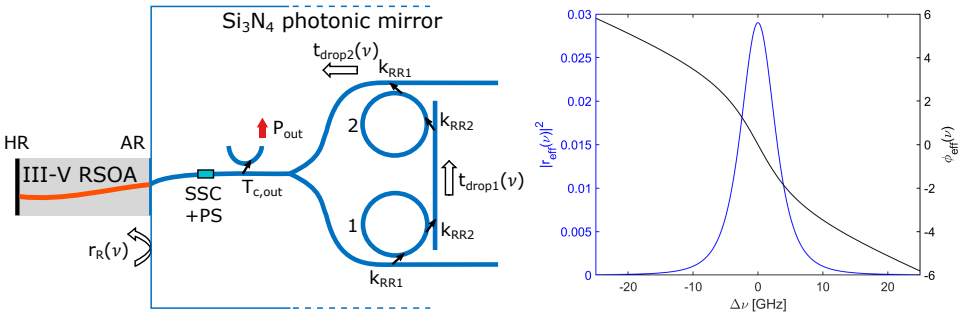

(a) (b)

Figure 1. (a) Scheme of the hybrid laser. (b) Effective reflectivity modulus square (left y-axis) and phase (right y-axis).

factor, and the effect of four-wave mixing are highlighted. These dynamical scenarios have been experimentally observed in similar structures[3,8] via the tuning of the laser emission frequency through a phase control section in the SiPh circuit, but were lacking a theoretical model able to explain in details their occurrence.

2. METHODS

We consider a hybrid laser consisting of a commercial III-V MQW HR/AR reflective SOA of 1 mm cavity length L that is edge-coupled to a SiPh mirror based on two Si_3N_4 coupled rings, as illustrated in Fig. 1(a). The ring design allows for an effective reflection coefficient ($|r_{eff}(\omega)|^2$) of 6 GHz FWHM bandwidth, with peak reflectivity 3%, as shown in Fig. 1(b). The power coupling coefficients are chosen as $k_{RR1} = k_{RR2}$ in order to maximize mirror reflection in the critical coupling regime. The output coupler power transmission coefficient $T_{c,out} = 73\%$ is designed to optimize the WPE at the output power of 20 mW.[9] When addressing the laser performance in presence of spurious back reflections, we add at the scheme in Fig. 1(a) an external reflector of reflection coefficient r_{ext}, placed at a distance L_{ext} from the output coupler. In the general case, the total reflectivity accounting for the SiPh mirror and the external optical feedback is

$$r_R(\omega) = r_{eff}(\omega) + t_{SSC}^2 T_{c,out} r_{ext} e^{-i\phi_{ext}} e^{-i\tau_{ext}(\omega-\omega_0)} = |r_R(\omega)| e^{i\phi_R(\omega)} \tag{1}$$

with t_{SSC} being the spot size converter transmission coefficient, τ_{ext} the external cavity delay, and $\phi_{ext} = 2L_{ext}\omega_0 n_{eff,SiN}/c$ with $n_{eff,SiN}$ the effective refractive index in the SiN platform and ω_0 the reference angular frequency. The considered model consists of a set of time-delayed algebraic differential equations[7,10] in the reference plane of the AR-coated facet of the RSOA. In particular, we combine an evolution equation for the output of the SOA $E(t)$, incident on the SiPh mirror (derived from the roundtrip equation[7]) with a standard rate equation for the carrier density, and two equations for the fields $A_{c1}(t)$ and $A_{c2}(t)$, respectively describing the output of the drop port of ring 1 and the output of the splitter after propagation in ring 2. Assuming that ring 1 and 2 are tuned to align both ring resonance wavelengths at $\omega_0 = 2\pi c/\lambda_0$ (with $\lambda_0 = 1310$ nm) and that the response of each ring can be approximated as a Lorentzian around ω_0, we obtain the following set of equations

$$\begin{aligned}
E(t) &= \frac{e^{i(\omega_s-\omega_0)\tau_{in}} \exp\left(\frac{1}{\tau_{in}}\int_{t-\tau_{in}}^{t} L\left(1+i\alpha\frac{\omega_s}{\omega_0}\right) g_N \ln\left(\frac{N(\bar{t})}{N_s}\right) d\bar{t}\right)}{r_R(\omega_s)} A^-(t-\tau_{in}) \\
&\quad + F(t) \qquad (2)\\
\frac{dA_{c1}(t)}{dt} &= \gamma_{c1} t_{SSC}\sqrt{1-T_{c,out}} E(t-\tau_{in,SiN}/2) e^{-i\Delta\phi/2} - \gamma_{t1} A_{c1}(t) \qquad (3)\\
\frac{dA_{c2}(t)}{dt} &= \gamma_{c2} A_{c1}(t) - \gamma_{t2} A_{c2}(t) \qquad (4)\\
\frac{dN(t)}{dt} &= \frac{\eta_i I}{qV} - \frac{N(t)}{\tau_N} - v_g g_N \ln\left(\frac{N(t)}{N_0}\right)\sigma\frac{|E(t)|^2}{V} \qquad (5)
\end{aligned}$$

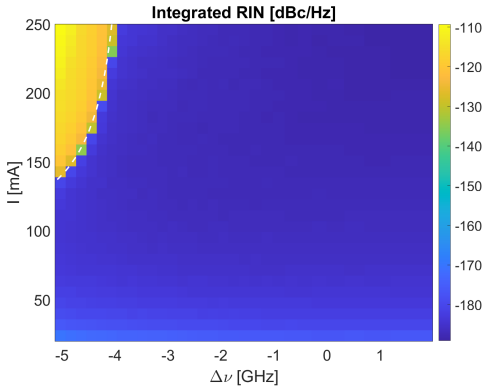

Figure 2. Map of the Relative Intensity Noise (RIN) integrated over a bandwidth of 25 GHz as a function of the RSOA bias current (y-axis) and the detuning of the lasing mode with respect to the effective reflectivity peak (x-axis). The white dashed line highlights the border of CW instability.

with

$$\begin{aligned} A^{-}(t-\tau_{in}) &= t_{SSC}\sqrt{1-T_{c,out}}e^{-i\Delta\phi/2}A_{c2}(t-\tau_{in}-\tau_{in,SiN}/2) \\ &\quad +t_{SSC}^{2}T_{c,out}r_{ext}e^{-i\phi_{ext}}E(t-\tau_{in}-\tau_{ext}) \end{aligned}$$

and the coefficients

$$\gamma_{c1,2}=\frac{v_{g1,2}k_{RR}}{2\pi R_{1,2}t_{RR}A_{loss1,2}^{1/4}} \qquad \gamma_{t1,2}=\frac{v_{g1,2}\left(1-t_{RR}A_{loss1,2}^{1/2}\right)}{2\pi R_{1,2}t_{RR}A_{loss1,2}^{1/2}}$$

accounting respectively for the rate at which the electric field is coupled into the ring and the rate at which the field is lost due to ring losses $A_{loss1,2}$ and coupling out to the bus waveguide. Here, $v_{g1,2}$ are the group velocities inside the two rings, $R_{1,2}$ the ring radii, and $t_{RR}=1-k_{RR}$.

We highlight the presence of a phase shift term $\Delta\phi$, introduced by the phase control section (PS), allowing the tuning of the lasing mode wavelength through the variation of the effective refractive index Δn_{eff} of an additional piece of waveguide of length L_{ps}. $F(t)$ in Eq. (2) accounts for spontaneous emission noise, α is the linewidth enhancement factor, g_N is the modal gain coefficient. In Eq. (5), η_i is the internal quantum efficiency, q is the electron charge, v_g is the group velocity in the RSOA, V is the active region volume, N_0 the carrier density value at transparency, and τ_N the carrier lifetime in the RSOA. $\tau_{in,SiN}$ is the time delay associated to the straight waveguide parts of the circuit, while τ_{in} is the RSOA cavity roundtrip time (more details can be found in a previous publication by some of the authors[9]).The coefficient σ accounts for the average of the electric field along propagation inside the RSOA.[7]

The effective reflection coefficient at the AR-coated facet of the RSOA, accounting for the SiPh mirror, can be calculated as

$$r_{eff}(\omega)=\frac{\gamma_{c1}\gamma_{c2}t_{SSC}^{2}(1-T_{c,out})}{(\gamma_{t1}+i\Delta\omega)(\gamma_{t2}+i\Delta\omega)}e^{-i\Delta\phi}e^{-i\Delta\omega\tau_{in,SiN}} \tag{6}$$

with $\Delta\omega=\omega-\omega_0$. The set of equations given by Eq. (2-5) enables efficient numerical simulations of the laser scheme, as well as the development of a linear stability analysis (LSA) of the CW solutions in the frequency domain,[7] which highlights the possible sources of CW instability. In particular, the two main complex roots of the linearized system determinant are associated to the relaxation oscillation resonance (RO) and photon-photon resonance (PPR). The real and imaginary part of the complex roots are respectively associated to the perturbation frequency and damping. Studying the evolution of the roots as a function of the dispersive mirror bandwidth, the tuning of the phase control section, and the external cavity reflectivity, allows to address the impact of these control parameters on CW stability in solitary laser operation and in presence of optical feedback.

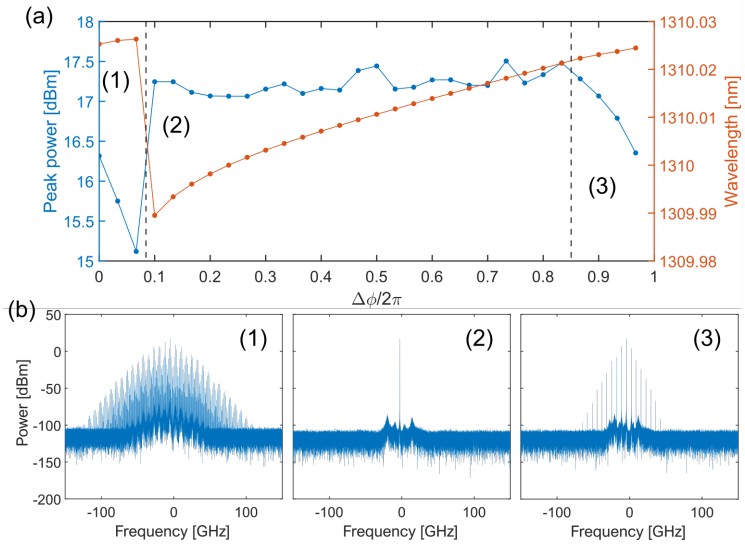

Figure 3. (a) Plot of the optical spectrum peak power (left y-axis) and the lasing wavelength (right y-axis) as functions of the phase detuning term $\Delta\phi$. (b) Optical spectra for region 1 (turbulent regime), region 2 (single-mode emission), and region 3 (regular self-pulsing oscillations).

3. RESULTS

3.1 Solitary laser

We first perform the analysis of the solitary laser for $r_{ext} = 0$. We report in Fig. 2 the map of the RIN, integrated over a bandwidth of 25 GHz as a function of the RSOA bias current and the detuning $\Delta\nu$ of the lasing frequency with respect to the effective reflectivity $|r_{eff}(\omega)|^2$ peak that can be varied by acting on the phase control section via $\Delta\phi$. Note that $\Delta\nu = 0$ corresponds to $\Delta\phi/2\pi \approx 0.23$. Here, the blue region of low RIN (i.e., associated to an integrated RIN lower than -150 dBc/Hz) corresponds to a stable regime with single-mode output (CW emission), while the yellow region of high RIN (i.e., associated to an integrated RIN higher than -130 dBc/Hz) corresponds to either a self-pulsing or turbulent regime. The white dashed line in Fig. 2, obtained through LSA, highlights the location of the zero isoline of the minimum imaginary part of the roots of the perturbation system determinant.[7] This line identifies the border between the stable and unstable CW regime (from positive to negative imaginary part of the roots). In analogy to what was done by Huang *et al.*,[3] we report in Fig. 3(a) the highest lasing wavelength and the optical spectrum peak power for varying $\Delta\phi$ at fixed RSOA bias current of 230 mA, and in Fig. 3(b) the optical spectra corresponding to region 1 (turbulent regime), region 2 (stable single-mode regime), and region 3 (self-pulsing regime). In order to interpret the transitions from the stable to the unstable regime, we use the results of LSA, reported in Fig. 4, where we show, in blue, the frequency (a) and damping rate (b) of the determinant root associated to ROs. In regions (1) and (3) in Fig. 3 of multimode emission the imaginary part of the RO root becomes negative (positive perturbation rate) and its real part, corresponding to the perturbation frequency, approaches the RO resonance. This means that the CW instability, evolving either towards self-pulsing or the turbulent regime, occurs when the beating between two neighboring longitudinal modes becomes resonant with the RO frequency and relaxation oscillations become undamped.

In particular, for negative detunings far from $\Delta\nu = 0$ GHz, the phase noise on the CW lasing mode caused by spontaneous emission turns into high intensity noise due to the narrow band reflector. Because of a non-null linewidth enhancement factor, this causes a variation in the carrier-induced refractive index and thus a shift of the longitudinal modes below the reflectivity curve. This effect may favour the reaching of the lasing threshold for the longitudinal mode nearest to the CW lasing mode (if longitudinal modes are close enough) and thus their beating. When the beating frequency is resonant with the RO frequency the multimode emission is sustained and, for sufficiently high bias current, mode proliferation is provided by the nonlinear frequency mixing phenomena (e.g., Four Wave Mixing). When this occurs, self-pulsing or turbulent regimes are observed depending on the value of $\Delta\nu$ and bias current. For smaller detunings we may argue that the detuned loading effect at the basis of

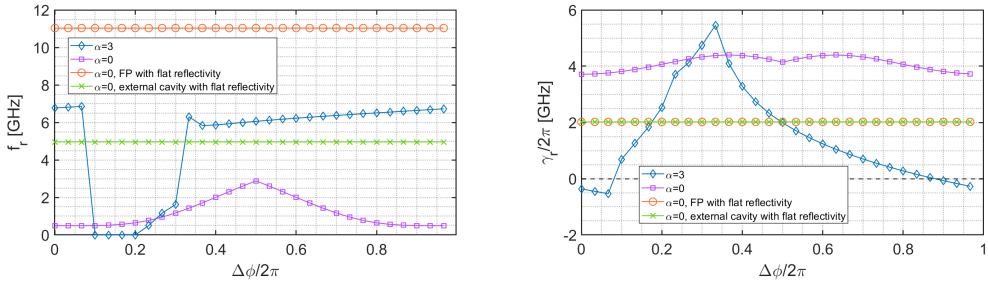

(a) (b)

Figure 4. (a) Frequency and (b) damping rate of the system determinant root associated to relaxation oscillation for $\alpha = 3$ (in blue) and $\alpha = 0$ (in violet). The orange and green curves represent the results of the corresponding system determinant in the case of a single-mode laser with flat reflectivity (in orange) and a single-mode laser with and external cavity and flat reflectivity (in green).

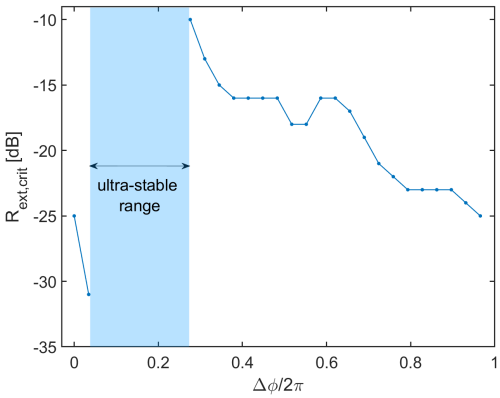

Figure 5. Critical feedback level as a function of the frequency shift $\Delta\phi$ for $L_{ext} = 0.5$ cm. The shaded region identifies an ultra-stable regime.

narrow linewidth emission in SiPh hybrid lasers,[4] opposes this process by reducing phase fluctuations of the CW mode. As consequence of this detuned loading effect, we report a maximum RO damping for CW emission close to the effective reflectivity peak, i.e. for -1 GHz< $\Delta\nu$ <-0.5 GHz (or $0.3 < \Delta\phi/2\pi < 0.37$, see Fig. 4(b)). In Fig. 4(a,b) we also show the frequency and damping of the perturbation associated to RO for $\alpha = 0$ (in violet), in the case of a standard "Fabry-Perot" (FP) single-mode cavity laser with mirror reflectivity independent on frequency (in orange), and in the case of an external cavity laser with frequency independent reflectivity (in green). We can observe that the $\alpha = 0$ case shows that the CW emission is always stable, thus demonstrating that in order to properly describe our hybrid laser, the impact of the α factor needs to be taken into account. Further, the two flat reflectivity cases show the same (constant) damping rate for RO and, in particular, display a lower damping rate near the optimal trade-off peak point of the blue curve, where relaxation oscillations are highly damped as an effect of the filter action exerted by the narrow band mirror. Finally, the value in frequency associated to the perturbation in the case of the external cavity laser with flat reflectivity is reduced by a factor $\sqrt{\tau_{in}/(\tau_{in} + \tau_{eff})}$ with τ_{eff} being the time delay of the external cavity.

3.2 Feedback tolerance

By studying how optical feedback affects the single mode laser stability, we identify the best parametric region for the design of feedback resilient SiPh hybrid laser. We consider a value of RSOA bias current at 104 mA (corresponding to an output power of ≈20 mW) and an external cavity length $L_{ext} = 0.5$ cm, considered as the typical distance from which we expect spurious back-reflections from the SiPh circuit. In Fig. 5 we report the critical feedback level $R_{ext,crit}$, i.e. the minimum value of the external reflectivity $R_{ext} = |r_{ext}|^2$ causing CW instability. Here, we can appreciate the presence of an ultra-stable region, where the hybrid laser is stable up

to a feedback level of -10 dB. Note that since the introduction of $r_{ext} \neq 0$ in Eq. (1) modifies the shape of the reflectivity, the actual lasing mode solution corresponding to the indicated $\Delta\phi$ differs in general from the solitary case, especially for non-negligible values of R_{ext}. As expected, the shaded ultra-stable region corresponds to values of the detuning $\Delta\nu$ around the maximum RO damping.

4. CONCLUSIONS

We have presented a model that can be employed to efficiently study the stability of a III-V SiN hybrid cavity laser with a dispersive narrow band mirror. Such model allows to account for the amplitude and phase dispersion of the mirror, the existence of several laser cavity longitudinal modes, and the detuning of the lasing frequency with respect to the mirror reflectivity peak. We have thus shown that narrow band mirrors are effective in damping the laser relaxation oscillations for stable CW emission in a range of detunings, although regimes of multimode emission can be also observed. Finally, we have identified an ultra-stable detuning range in presence of spurious back-reflections, allowing for possible applications in the design of isolator-free laser sources.

ACKNOWLEDGMENTS

This work is supported under a CISCO Sponsored Research Agreement. The authors acknowledge Dr. Fabrizio Forghieri (Cisco Photonics, Vimercate, Italy) for coordinating the project.

REFERENCES

[1] Komljenovic, T., Srinivasan, S., Norberg, E., Davenport, M., Fish, G., and Bowers, J. E., "Widely tunable narrow-linewidth monolithically integrated external-cavity semiconductor lasers," *IEEE Journal of Selected Topics in Quantum Electronics* **21**, 214–222 (Nov 2015).

[2] Fan, Y., Lammerink, R. E. M., Mak, J., Oldenbeuving, R. M., van der Slot, P. J. M., and Boller, K.-J., "Spectral linewidth analysis of semiconductor hybrid lasers with feedback from an external waveguide resonator circuit," *Opt. Express* **25**, 32767–32782 (Dec 2017).

[3] Huang, D., Tran, M. A., Guo, J., Peters, J., Komljenovic, T., Malik, A., Morton, P. A., and Bowers, J. E., "High-power sub-khz linewidth lasers fully integrated on silicon," *Optica* **6**, 745–752 (Jun 2019).

[4] Tran, M. A., Huang, D., and Bowers, J. E., "Tutorial on narrow linewidth tunable semiconductor lasers using si/iii-v heterogeneous integration," *APL Photonics* **4**(11), 111101 (2019).

[5] Fan, Y., van Rees, A., van der Slot, P. J. M., Mak, J., Oldenbeuving, R. M., Hoekman, M., Geskus, D., Roeloffzen, C. G. H., and Boller, K.-J., "Hybrid integrated inp-si3n4 diode laser with a 40-hz intrinsic linewidth," *Opt. Express* **28**, 21713–21728 (Jul 2020).

[6] Xiang, C., Jin, W., Guo, J., Williams, C., Netherton, A. M., Chang, L., Morton, P. A., and Bowers, J. E., "Effects of nonlinear loss in high-q si ring resonators for narrow-linewidth iii-v/si heterogeneously integrated tunable lasers," *Opt. Express* **28**, 19926–19936 (Jul 2020).

[7] Detoma, E., Tromborg, B., and Montrosset, I., "The complex way to laser diode spectra: example of an external cavity laser strong optical feedback," *IEEE Journal of Quantum Electronics* **41**(2), 171–182 (2005).

[8] Mak, J., van Rees, A., Fan, Y., Klein, E. J., Geskus, D., van der Slot, P. J. M., and Boller, K.-J., "Linewidth narrowing via low-loss dielectric waveguide feedback circuits in hybrid integrated frequency comb lasers," *Opt. Express* **27**, 13307–13318 (Apr 2019).

[9] Columbo, L., Bovington, J., Romero-Garcia, S., Siriani, D. F., and Gioannini, M., "Efficient and optical feedback tolerant hybrid laser design for silicon photonics applications," *IEEE Journal of Selected Topics in Quantum Electronics* **26**, 1–10 (March 2020).

[10] Tromborg, B., Olesen, H., Pan, X., and Saito, S., "Transmission line description of optical feedback and injection locking for fabry-perot and dfb lasers," *IEEE Journal of Quantum Electronics* **23**(11), 1875–1889 (1987).